Rotational spectra of the carbon-chain radicals HC_5O, HC_6O, and HC_7O

S. Mohamed and M. C. McCarthy[a)]
Harvard-Smithsonian Center for Astrophysics, 60 Garden Street, Mail Stop 72, Cambridge, Massachusetts 02138 and Division of Engineering and Applied Sciences, Harvard University, Cambridge, Massachusetts 02138

A. L. Cooksy and C. Hinton[b)]
Department of Chemistry, San Diego State University, 5500 Campanile Drive, San Diego, California 92182

P. Thaddeus
Harvard-Smithsonian Center for Astrophysics, 60 Garden Street, Mail Stop 72, Cambridge, Massachusetts 02138 and Division of Engineering and Applied Sciences, Harvard University, Cambridge, Massachusetts 02138

(Received 2 September 2005; accepted 28 September 2005; published online 16 December 2005)

Three new free carbon-chain radicals, HC_5O, HC_6O, and HC_7O, and their deuterated isotopic species have been observed by Fourier transform microwave spectroscopy of a supersonic molecular beam. In contrast to the shorter HC_nO radicals, these all have linear heavy-atom backbones and $^2\Pi$ electronic ground states. Like the isovalent HC_nS radicals, the ground states of the HC_nO radicals alternate with odd and even numbers of carbon atoms: those of HC_5O and HC_7O are $^2\Pi_{1/2}$ and that of HC_6O is $^2\Pi_{3/2}$. From frequency measurements between 6 and 26 GHz, the rotational constant B, the centrifugal distortion constant D, and the lambda-type doubling and magnetic hyperfine constants have been determined to high precision for each chain. Predicted properties from coupled-cluster calculations are also reported for chains up to HC_9O. The production of HC_nO radicals for n even was highly favored when O_2 was used as the source of oxygen, but those with n odd were best produced with CO. © *2005 American Institute of Physics*. [DOI: 10.1063/1.2126970]

I. INTRODUCTION

Carbon-chain radicals terminated with oxygen are thought to be important intermediates in combustion processes,[1,2] photofragmentation of stable molecules,[3] and interstellar chemistry.[4,5] Because these radicals are also subject to the Renner-Teller effect,[6] which depending on the strength of the vibronic interaction results in either bent or linear ground state geometries, their structure and spectroscopic properties are of interest. The first four members of the HC_nO series have been studied by rotational spectroscopy; each possesses a rotational spectrum characteristic of a nonlinear, nearly prolate asymmetric top. All have planar structures, but the location along the heavy-atom backbone where the molecule is bent and the bending angle differ in each chain: the angle is 120° for HCO;[7] the H–C–C angle is 140° for HCCO;[8] the C–C–O angle is 136° for HC_3O;[9] and the H–C–C angle is probably close to 160° for HC_4O.[10] The structure and spectroscopic constants of HC_5O and longer chains have not been determined by experiment or calculated by *ab initio* methods prior to the present work.

Here we report the laboratory detection in a supersonic molecular beam with a Fourier transform microwave (FTM) spectrometer of the next three members of the HC_nO series: HC_5O, HC_6O, and HC_7O (Fig. 1). Relative energies, dipole moments, and equilibrium geometries for this series of carbon chains to HC_9O have been predicted by *ab initio* calculations. In contrast to the shorter chains, these here have linear or nearly linear heavy-atom backbones and $^2\Pi$ electronic ground states. Both HC_5O and HC_7O have regular fine structure, with the $^2\Pi_{1/2}$ ladder the lower in energy, while HC_6O has an inverted fine structure, with the $^2\Pi_{3/2}$ ladder the lower in energy. For each radical, at least seven rotational transitions were measured in the lowest fine-structure ladder in the centimeter-wave band (6 and 26 GHz), and spectroscopic constants, including those that describe the lambda-type doubling and hyperfine structure from the hydrogen atom, have been determined to high precision. About ten rotational transitions of the deuterated isotopic species of each radical have also been detected, yielding spectroscopic constants in close agreement with those expected.

The production of the radical chains from HC_3O to HC_7O has also been investigated, with various precursor gases as the source of oxygen. The lines of all five chains were observed either in an O_2 or CO discharge, but the lines were typically ten times weaker in one through CO_2. In addition, large variations in the relative abundances of chains with odd and even numbers of carbon atoms beyond HC_3O were observed when O_2 or CO were used: odd-numbered chains are produced ten times more abundantly with CO than with O_2, while even-numbered chains are produced ten times more abundantly with O_2 than with CO. A simple formation

[a)]Electronic mail: mccarthy@cfa.harvard.edu
[b)]Present address: Department of Chemistry, University of Utah, Salt Lake City, Utah 84112.

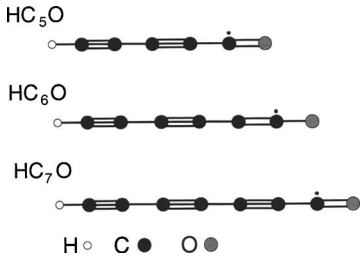

FIG. 1. The carbon-chain radicals HC_5O, HC_6O, and HC_7O. The valence structures shown are only approximate since several resonance structures presumably contribute to the $^2\Pi$ electronic ground states.

mechanism to explain this difference is the reaction $HC_{2n}+CO(O_2)\rightarrow HC_{2n+1}O(HC_{2n}O+O)$. Similar investigations of the formation of HC_3O by Cooksy *et al.*[9] and HC_4O by Kohguchi *et al.*[10] are consistent with our observations.

II. EXPERIMENT

The three radicals here and their deuterated isotopic species were detected in the discharge products of an organic vapor heavily diluted in neon. The discharge nozzle in the present experiment consists of a commercial solenoid valve (1 mm orifice) and alternating layers of Teflon insulators and Cu electrodes in which the orifice size is stepped up to 5 mm just prior to adiabatic expansion.[11] The nozzle is positioned in one of the mirrors of the confocal Fabry-Perot cavity of the spectrometer, a configuration which yields very sharp lines and allows line frequencies to be determined up to the order of one part in 10^7. By applying a potential of at least 600 V between the two Cu electrodes, a small discharge is struck in the throat of the nozzle. Fragmentation of the precursor followed by rapid reactions efficiently forms longer carbon chains, including many highly reactive polyenes, radicals, and cumulene carbenes.[12] The thermodynamic and kinetic processes which govern molecule formation are poorly understood, so the optimal conditions for production must be determined empirically.

As molecules expand from the discharge nozzle into the Fabry-Perot cavity, rotational energy is rapidly converted to translational energy via collisions with the inert buffer gas. Within a short distance (approximately a few tens of nozzle diameters) from the nozzle, the effective rotational temperature drops to only 2–3 K and the velocity of the beam reaches about twice the speed of sound in air, i.e., ~700 m/s. As the molecules approach the center of the cavity, a short 1 μs pulse of microwave radiation at frequency ν_0 is applied. The Fourier transform of the free induction decay yields the power spectrum, which is then displayed as a frequency offset from the pump frequency ν_0. To achieve narrow linewidths and high spectral resolution for radical species, three mutually perpendicular sets of Helmholtz coils are used to cancel the Earth's magnetic field at the center of the cavity. The residual magnetic field was about 10–15 mG (about 3% of the zeroth-order field of 400 mG) over the active volume of the spectrometer, sufficiently small to allow resolution of closely spaced hyperfine structure (hfs) but still large enough to broaden some of the lower rotational transitions by more than the intrinsic instrumental linewidth of ~6 kHz that arises mostly from the time-of-flight of the molecular beam[13] through the Fabry-Perot cavity.

The experimental conditions used to detect HC_5O and the two longer chains were those that produced strong lines of either HC_3O (Ref. 14) or HC_4O:[10] a gas pulse of 280–300 μs duration, yielding a flow of 25–35 cm^3/min at STP, a stagnation pressure behind the nozzle of 2.5 kTorr (3.2 atm), and a discharge voltage of 800–1000 V. HC_3O required the lowest voltage, while longer chains required an additional ~50 V per carbon atom. The gas mixtures that produced the strongest lines of HC_3O and those of the two longer odd-numbered chains were HC_4H (0.15%) and CO (0.2%) in Ne; the lines of HC_4O and HC_6O were strongest when O_2 (0.4%) was used instead of CO. CO_2 was also used as a source of oxygen, instead of CO and O_2, but the lines of HC_3O and the four longer chains were then systematically fainter by an order of magnitude. The relative abundance of the HC_nO chains ($n>2$) using different hydrocarbon and oxygen precursor gases is discussed in detail in Sec. IV C. Using the best precursor gases, the strongest hyperfine split lines of HC_5O and HC_6O were observed with signal-to-noise ratios of greater than 30 in 1 min of integration, but about 10 min of integration were required to observe the comparably strong lines of HC_7O.

Line searches were guided by rotational constants predicted at the QCISD/cc-pVDZ level of theory (Sec. III). At both the QCISD and uhf levels, HC_6O and HC_7O are predicted to possess linear geometries, but for HC_5O the two predict different structures: uhf predicts a linear geometry, but QCISD predicts a bent geometry. Since previous searches for bent HC_5O had been unsuccessful in this laboratory, a wide search (±4% around the predicted frequencies) was undertaken assuming that HC_5O possesses a linear geometry and a $^2\Pi$ ground state. Four closely spaced magnetic lines were eventually found at about 3.2% in frequency above the theoretical prediction, which on the basis of additional spectroscopic measurements and assays were quickly shown to be HC_5O. Searches for the next two radicals were based on scaled *ab initio* calculations in which the theoretical rotational constants were scaled up by 1.032, the ratio of the experimental rotational constant to that calculated at the same level of theory for HC_5O. Rotational transitions of both radical chains were observed within ±0.4% of these predictions.

The spectroscopic and chemical evidence in support of the present identifications is very strong. For HC_5O and the two longer chains, the experimental rotational constants are in good agreement with those predicted by theory. Theory systematically underestimates the measured rotational constants by about 3%, but this result is consistent with vibrational effects, since on bending the vibrationally averaged experimental geometries are more compact than the equilibrium geometries. When the theoretical rotational constant is scaled to the experimental value for HC_5O, the agreement for HC_6O and HC_7O is extremely good, i.e., the predicted and experimental rotational constants agree to 0.4% and 0.1%, respectively. The centrifugal distortion constants D of the three new chains are also close to those of the closely related C_nH radicals of similar size.[15] The absence of lines at

TABLE I. UQCISD/cc-pVDZ properties of HC_nO stationary-point geometries.

Molecule	State	Geometry[a]	$\langle S^2\rangle_{uhf}$	ΔE[b] (kJ/mol)	$(B+C)/2$ (GHz)	μ (D)
HCO	$^2A'$	$\theta_{HCO}=124°$	0.76	0.0	42.59	1.51
	$^2\Pi$	Linear	0.78	[118]	39.14	2.27
HC_2O	$^2A''$	$\theta_{HCC}=129°$	0.82	0.0	10.62	1.48
	$^2\Pi$	Linear	0.84	[11.2]	10.53	1.90
HC_3O	$^2A'$	$\theta_{CCO}=134°$	1.03	0.0	4.454	2.40
	$^2A'$	$\theta_{HCC}=139°$	1.20	12.7	4.355	1.41
	$^2\Pi$	Linear	1.12	[27.0]	4.268	2.08
HC_4O	$^2A''$	$\theta_{CCC(O)}=140°$[c]	1.12	0.0	2.318	1.73
	$^2\Pi$	Linear	1.19	[4.1]	2.166	2.04
HC_5O	$^2A'$	$\theta_{CCO}=133°$	0.90	0.0	1.272	2.68
	$^2A'$	$\theta_{CCC(O)}=160°$[c]	1.64	9.1	1.263	2.14
	$^2\Pi$	Linear	1.61	[10.3]	1.253	2.16
HC_6O	$^2A''$	$\theta_{CCC(O)}=138°$[c]	1.61	0.0	0.845	1.77
	$^2\Pi$	Linear	1.71	[3.8]	0.791	2.11
HC_7O	$^2\Pi$	Linear	2.13	0.0	0.532	2.17
HC_8O	$^2A''$	$\theta_{CCC(O)}=138°$[c]	2.14	0.0	0.394	1.84
	$^2\Pi$	Linear	2.25	[3.3]	0.375	2.19
HC_9O	$^2\Pi$	Linear	2.16	0.0	0.275	2.67

[a]Unless otherwise indicated, the HCC unit, the carbon-chain backbone, and the CCO unit are found to be linear or nearly linear.
[b]Energy in brackets indicates a saddle-point geometry.
[c]Indicates the bond angle of the CCC unit adjacent to the oxygen atom.

subharmonic frequencies indicates that the carriers of the observed lines cannot be from larger or heavier molecules, and because the lines are harmonically related by half-integer quantum numbers, the carriers of the assigned lines are radicals. In addition, the rotational spectra of the three chains exhibit a resolved structure owing to lambda-doubling in a $^2\Pi$ state and hfs which arises from the interaction of the nuclear spin of hydrogen with the unpaired electron. The lambda-doubling constants ($p+2q$ for HC_5O and HC_7O and q for HC_6O) and the hyperfine constants (a_-, b, and d for HC_5O and HC_7O, and a_+ and b for HC_6O) for each chain are close to those of similar-sized C_nH radicals, indicating that the electronic structure and bonding are apparently not significantly altered when oxygen terminates the carbon chain.

The observed lines also pass several other tests: they are only observed in the presence of an electrical discharge through gases containing hydrogen, carbon, and oxygen. The behavior of the lines in the presence of a small magnetic field is consistent with the assigned ground state of each molecule: the lines of HC_5O and HC_7O are not modulated by a magnetic field of a few gauss, confirming that this state does not possess a large magnetic moment, as expected for a $^2\Pi_{1/2}$ state near the Hund's coupling case (a) limit. The lines of HC_6O, however, are readily modulated with the same magnetic field, as expected for a radical with a $^2\Pi_{3/2}$ ground state. Finally, conclusive confirmation of the assignments is provided by isotopic substitution: lines of deuterated isotopic species were observed within 0.2% of those predicted by scaling from the normal species of each chain.

III. COMPUTATIONAL DETAILS

Equilibrium geometries were optimized for HCO through HC_9O at the UQCISD level using Dunning's cc-pVDZ basis set. For molecules with nonlinear equilibrium structures, partial optimizations were also carried out on linear geometries. Complete active space self-consistent-field (CASSCF) calculations were also carried out to confirm the equilibrium geometries and to estimate spin-orbit coupling constants using the full Breit-Pauli Hamiltonian. The CASSCF active spaces were selected to correspond to a balanced set of π bonding and antibonding orbitals in the linear molecule limit, for a total of $2n+3$ electrons in as many orbitals up to $n=5$. For HC_6O and HC_8O, the active space was limited to 11 electrons in 11 orbitals (11,11), and for HC_7O and HC_9O, a (13,13) active space was used. Harmonic frequency analyses were performed on HC_4O and HC_5O, and single-point calculations were also carried out at the UCCSD(T)/cc-pVDZ level and at the UQCISD/cc-pVTZ level, to assess the extent of convergence with respect to higher-order substitutions and basis-set size. The GAMESS suite of programs[16] was used for all restricted open-shell Hartree-Fock (ROHF)-based calculations and GAUSSIAN 98[17] for the UHF-based calculations; both programs were run on a variety of Intel, Compaq, HP, and SGI Unix workstations.

The results of the UQCISD analysis are summarized in Table I. Spin contamination of the UHF reference wave functions becomes increasingly severe as the chain lengthens and

the perturbing quartet states become more stable. Although the coupled-cluster treatment substantially corrects for the spin-mixed reference, the validity of the unrestricted treatment is sorely tested in the eight- and nine-carbon chains, for which the UHF wave functions approach 50% contamination. The qualitative features of this analysis, however, particularly the shapes of the equilibrium geometries, are supported by the uncontaminated CASSCF calculations. The impact of spin contamination is felt more strongly on relative energies of electronic states than on equilibrium geometries; (contamination aside) UHF wave functions routinely model electron distributions and relative energies in radicals more accurately than the more constrained ROHF wave functions. Because coupled-cluster calculations have yielded good agreement with spectroscopic parameters in this series of molecules previously,[18] superior to CASSCF calculations of similar computational intensity, the UQCISD results are quoted in Table I.

The relative energies of the nonequilibrium stationary points cited in Table I are very likely to be too high by 2–5 kJ/mol, although we do not expect any to be inverted. Zero-point energy corrections and larger basis sets tend to lower these energies, based on the results obtained for $n<6$.

As expected from the canonical forms of the HC_nO molecules, the series breaks into two subgroups: the even n molecules, which tend towards $^2A''$ ground states that bend at the HCC subunit or at the carbon adjacent to the CO subunit, and the odd n molecules, favoring $^2A'$ ground states that bend at the CCO subunit. Both subgroups are also subject to an overall trend that lowers the barrier to linearity with increasing chain length. Analysis of these trends in the electron distribution as a function of chain length have been discussed in previous papers, most recently in our work on the NC_nS series.[19] Those considerations remain in force for this series, with the added complication of a C–H bond in place of the nitrogen atom in NC_nS (so odd n in the HC_nO series corresponds to even n in NC_nS and vice versa).

The barriers to linearity shown in Table I strongly suggest that beyond HC_5O the molecules are essentially quasilinear, despite the significant bending angle of 138° at the equilibrium geometries of HC_6O and HC_8O. The correspondingly low vibrational frequencies in these long chains may, nonetheless, keep the molecular geometries nonlinear on average in their ground vibrational states. While HC_7O and HC_9O are both predicted to have linear equilibrium geometries, the potential-energy surface is fairly flat along the CCO bending angle at the ROHF level, predicting large-amplitude bending.

The CASSCF spin-orbit constants A_{so}, listed in Table II, correspond to the matrix element coupling the A' and A'' states of the Renner-Teller couplet in the nonlinear molecules and to the term splitting of the $^2\Pi$ electronic state for the linear cases of HC_7O and HC_9O. The highest values are for HCO, HC_3O, and HC_5O, which strongly localize the spin density near the oxygen atom. As the spin density becomes more closely tied to the carbon chain, either with the even-n species or the longer-chain odd-n species, the spin-orbit constant drops by a factor comparable to the fourfold drop in A_{so} between ^3P atomic oxygen and ^3P atomic carbon.

TABLE II. CASSCF spin-orbit and spin-rotation coupling constants of HC_nO.

Molecule	A_{so} (cm^{-1})	ϵ_{aa}[a] (GHz)
HCO	71.0	4.3
HC_2O	38.0	16.0
HC_3O	59.8	1.3
HC_4O	36.3	2.7
HC_5O	52.8	1.0
HC_6O	22.4	0.5
HC_7O	22.0	
HC_8O	22.6	0.3
HC_9O	22.6	

[a]Spin-rotation constants are estimated from the Curl relation (Ref. 20) using the CASSCF A_{so} and ΔE values and the UQCISD A rotational constant.

For the long chains, however, it will probably be harder to measure A_{so} than the spin-rotation constant ϵ_{aa}, which correlates to A_{so} in the linear molecule limit. These two constants have been related by Curl[20] to the A rotational constant and the Renner-Teller energy gap ΔE: $\epsilon_{aa}=4AA_{so}/\Delta E$. The resulting values, given in Table II, are probably useful only for predicting trends. The methods employed for the A_{so} calculations reproduce atomic spin-orbit constants to within 20%, but the electronic energy calculations that yield ΔE are less accurate, since the value of the A rotational constant is imprecise for nearly linear molecules, and the Curl relation itself is very approximate. The spin-rotation constant is a sensitive function of the bending angle, and in these molecules even the zero-point bending amplitude is likely to extend over tens of degrees. In particular, the values for ϵ_{aa} in Table II underestimate the experimental values for HC_2O (−248 GHz) and HC_3O (11 GHz) by roughly an order of magnitude, consistent with a substantial contribution from more linear geometries.

The significance of ϵ_{aa} to the present work is that its value, relative to BJ, determines whether the observed spectrum is characteristic of Hund's case (a) or case (b) coupling. Even if the ϵ_{aa} values derived here are multiplied by a factor of 10, only HC_7O and HC_9O are predicted to have a case (a) coupling beyond J of about 10.

IV. RESULTS AND DATA ANALYSIS

A. HC_5O and HC_7O

Each of the lower rotational transitions of HC_5O and HC_7O is split into six components by substantial lambda-doubling of about 2 MHz and smaller hfs of about 0.2 MHz from the hydrogen atom. At least eight rotational transitions of both radicals fall within the frequency range of our FTM spectrometer; our measurements of these and of DC_5O and DC_7O can be obtained electronically through the Electronic Physics Auxiliary Publication Service (EPAPS).[21] A sample FTM spectrum of HC_5O is shown in Fig. 2. Transitions from the higher-lying $^2\Pi_{3/2}$ fine-structure ladder were not ob-

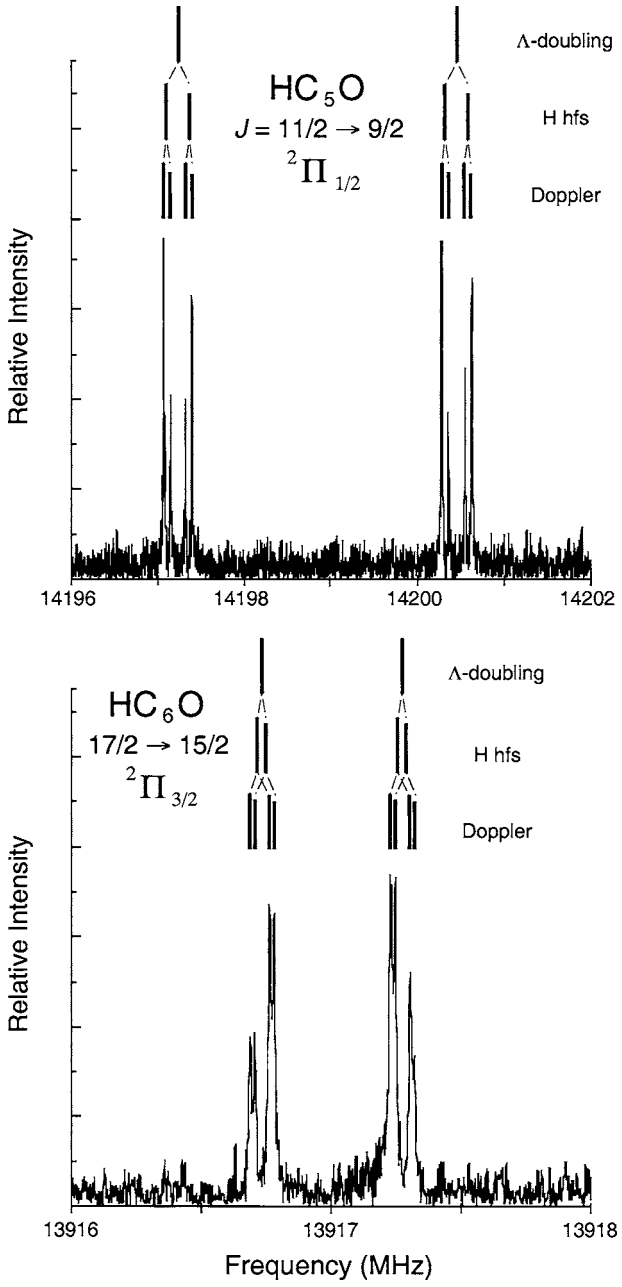

FIG. 2. Sample spectra of HC_5O and HC_6O showing Λ doubling, hydrogen hfs, and the double-peaked line profile. The line profile is instrumental in origin: it is the result of the Doppler shift of the Mach 2 molecular beam relative to the two traveling waves that compose the confocal mode of the Fabry-Perot. The integration time was approximately 2 min/MHz for both spectra.

served, because these lie at least 20 K above the ground-state transitions, and are not appreciably populated in our rotationally cold molecular beam (T_{rot}=2–3 K).

The standard Hamiltonian for a molecule in a $^2\Pi$ electronic state[22–24] was fitted to the measured frequencies. With the fine-structure constant A constrained at 20 cm^{-1} (27.6 K), about that of atomic carbon,[25] at most seven spectroscopic constants, the rotational constant B, the centrifugal distortion constant D, two lambda-doubling constants $p+2q$ and $(p+2q)_D$, and three hyperfine constants [the diagonal term $a_-=a-(b+c)/2$, the off-diagonal term b, and the Λ-doubling term d], were required to reproduce the data to an accuracy better than 3 kHz for each molecule. Because $A \gg 2BJ$ for the rotational levels observed to date, the Hund's case (a) combinations of $p+2q$ and q have been fitted, instead of p and q, separately. The spectroscopic constants so obtained are given in Tables III and IV.

B. HC_6O

The rotational spectrum of HC_6O is similar to that of HC_5O, but the structure from lambda-doubling and hydrogen hfs is smaller by a factor of 3 or more. Hfs is especially small, of the order of 10 kHz, but is still resolved because of the high spectral resolution (~3 kHz) achieved with our molecular beam aligned along the Fabry-Perot axis. Measured transition frequencies again are available electronically through the EPAPS;[21] a sample spectrum of HC_6O is shown in Fig. 2. The measurements were analyzed for HC_5O and HC_7O, but A was constrained to −20 cm^{-1}, owing to inverted fine structure. Five parameters were required to reproduce the experimental data to a rms better than 3 kHz for each species: B, D, q, and the hyperfine coupling constants $a_+=a+(b+c)/2$ and b. As demonstrated for other carbon-chain radicals,[26] the contribution of b to the observed hfs is not negligible and, as a result, the hfs collapses more slowly with increasing J than is expected from $a+(b+c)/2$ alone; if b is constrained to zero in the HC_6O fit, the rms increases by a factor of 4, from 1 to 4 kHz, and small, but systematic deviations in the fit residuals (O–C) are apparent. The spectroscopic constants for the normal isotopic species are given in Table III, those for the deuterated species are given in Table IV.

C. Formation of the HC_nO radicals

The abundance of HC_3O and the four longer oxygen-containing chains here depends somewhat on the hydrocarbon in the gas mixture, but is highly dependent on the source of oxygen. To better quantify the production of these molecules with different precursor gases, relative abundances were derived from intensity measurements using acetylene or diacetylene in combination with CO or O_2. To minimize possible variations in instrumental gain, transitions as close together in frequency as possible were measured for each radical. Relative abundances versus chain length are shown in Fig. 3.

It is apparent from Fig. 3 that, with the possible exception of HC_3O, the production of HC_nO radicals with n even is highly favored with oxygen, whereas radicals with n odd are best produced with CO, irrespective of the hydrocarbon source. Our findings confirm the previous observations of Kohguchi *et al.*,[10] who noted that $HCCH/O_2$ yields strong lines of HCCO and HC_4O and that the relative line intensities of HC_4O using $HCCH/O_2$ and HCCH/CO differed by about a factor of 20. Although the abundance of HC_3O and HC_4O is similar with HCCH/CO, this decrement does not hold for longer chains: HC_5O is much more abundant than HC_4O, HC_6O is much less abundant than HC_4O, and HC_7O is produced in comparable abundance to HC_4O.

This odd-even alternation in abundance is particularly pronounced with acetylene. With the exception of HC_3O,

TABLE III. Spectroscopic constants of HC_5O, HC_6O, and HC_7O.

	HC_5O		HC_6O		HC_7O	
Constant[a]	Experiment	Predicted	Experiment	Predicted	Experiment	Predicted
A	600 000[b] ($20\ cm^{-1}$)		−600 000[b] ($-20\ cm^{-1}$)		600 000[b] ($-20\ cm^{-1}$)	
B	1293.6046(1)	1253[c]	819.767 92(6)	816.6[d]	549.205 38(3)	549.2[d]
10^6D	36(1)	41[e]	26.3(2)	11.3[f]	4.08(7)	4.7[g]
$p+2q$	2.986(5)	3.65[h]	⋯		0.538(3)	1.268[f]
$10^3(p+2q)_D$	1.71(3)		⋯		0.058(4)	
q	⋯		−0.9208(8)	−1.46[e]	⋯	
$a-(b+c)/2$	12.4(4)	16.2[h]	⋯		9.3(7)	10.2[f]
$a+(b+c)/2$	⋯		0.1(5)	0.4[e]	⋯	
b	−21.3(7)	−29[h]	−16(1)	−17[e]	−12(1)	−19[f]
d	9.2(2)	10.7[h]	⋯		5.8(7)	6.3[f]

[a]Units are in MHz. Uncertainties (in parentheses) are 1σ in the last significant digit.
[b]Fixed.
[c]Computed at the QCISD/cc-pVDZ level of theory.
[d]Scaled from rotational constant calculated at the QCISD/cc-pVDZ level of theory (see text).
[e]From C_6H (Ref. 15).
[f]From C_7H (Ref. 15).
[g]From C_8H (Ref. 26).
[h]From C_5H (Ref. 15).

which is produced in similar abundance from either $HCCH/O_2$ or HCCH/CO, the abundance of longer chains decreases by at least an order of magnitude when CO is used instead of O_2 or vice versa. The mixture of HCCH/CO, for example, produces only about 1/10 as much HC_4O and HC_6O as the $HCCH/O_2$ mixture, while the opposite is true for HC_5O and HC_7O. Diacetylene was also tested and was generally found to produce higher concentrations than acetylene. The abundance is fairly flat with chain length from HC_3O to HC_6O using HC_4H/O_2 and, with the exception of HC_5O, the same is also true with HC_4H/CO. HC_5O is very abundantly produced with HC_4H/CO, by more than a factor of 20 compared to any other chain.

A simple formation mechanism which can account for much of the variation in production in our discharge source is the addition reaction $HC_{2n}+CO(O_2)+M \rightarrow HC_{2n+1}O(HC_{2n}O+O)+M$, where M is a third body. The role of odd-numbered $C_{2n+1}H$ chains in HC_nO formation is assumed to be minor. This mechanism implies that abundances obtained with CO should be nearly identical to those obtained with O_2, but shifted up by one carbon atom. That is what is observed for HCCH, but for HC_4H, although the same general trend holds, the chemistry is apparently somewhat more complex. Previous studies by Lander *et al.*[2] demonstrated that the addition reaction $HC_2+CO+M \rightarrow HC_3O+M$ accounts for the observed CCH depletion when HCCH is flash photolyzed in the presence of CO. Isotopic studies of HC_3O formed via acetylene and CO (Ref. 9) in this laboratory also confirm the important role of this reaction in mol-

TABLE IV. Spectroscopic constants of DC_5O, DC_6O, and DC_7O (in MHz).

	DC_5O		DC_6O		DC_7O	
Constant[a]	Experiment	Expected[b]	Experiment	Expected[b]	Experiment	Expected[b]
A_{eff}	600 000[c] ($20\ cm^{-1}$)		−600 000[c] ($-20\ cm^{-1}$)		600 000[c] ($20\ cm^{-1}$)	
B	1235.064 74(3)	1233.33	788.409 97(4)	788.44	531.035 90(1)	531.03
10^6D	36[d]		23.6(1)		4[d]	
$p+2q$	2.866(4)	2.85	⋯		1.496(3)	1.49
$10^3(p+2q)_D$	1.60(2)		⋯		0.045(4)	
q	⋯		−0.8848(6)	−0.8524	⋯	
$a-(b+c)/2$	2.0(2)	1.9	⋯		1.3(5)	1.4
b	−3.5(4)	−3.3	⋯		−4.4(8)	−1.8
d	1.43(6)	1.41	⋯		0.5(2)	0.9

[a]Units are in MHz. Uncertainties (in parentheses) are 1σ in the last significant digit.
[b]Scaled from the normal isotopic species.
[c]Fixed.
[d]Fixed at the value of the normal isotopic species.

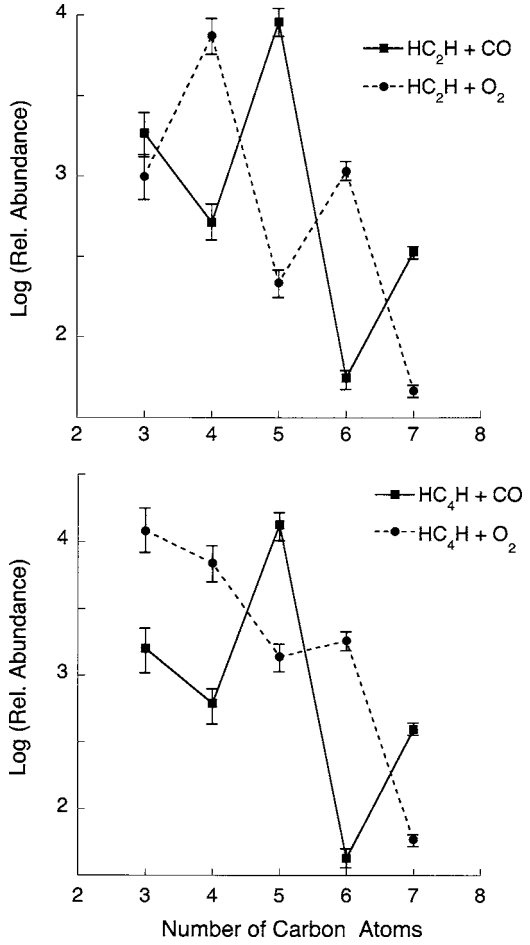

FIG. 3. Relative abundances of the HC_nO radicals per gas pulse in the supersonic molecular beam as a function of chain length. The abundances were derived from relative intensity measurements, correcting for the rotational partition function, line strength, and dipole moment (see Table I). The error bars represent the percent difference in the derived abundances using two different rotational transitions of each chain.

ecule formation: experiments with ^{13}CO indicate that roughly one-half of the HC_3O is formed without breaking the CO bond.

The similarly high abundance of both HC_4O, using HC_4H/O_2, and HC_5O, using HC_4H/CO and HC_6O (with O_2) and HC_7O (with CO), are consistent with molecule formation via addition. For other chains, however, the correlation between the HC_nO abundances using CO and O_2 is generally poor, a possible indication that other formation mechanisms are operative, and that these are at least somewhat nonspecific with respect to the number of carbon atoms. Reactions involving odd-numbered $C_{2n+1}H$ chains, for example, may be important. C_5H is known to be more than 50 times more abundant than C_6H in a HC_4H discharge,[27] so even if reactions with CO or O_2 are somewhat inefficient, these reactions may yield significant quantities of the HC_nO chains.

V. DISCUSSION

Although the shorter members of the HC_nO series ($n=1-3$) are subject to a strong Renner-Teller interaction, which results in planar, but nonlinear geometries for the electronic ground states, this interaction is apparently fairly weak for longer members of the series because the orbital angular momentum is not quenched. As a result, these radicals are linear with $^2\Pi$ electronic ground states. The closely related NC_nS radicals ($n=1-7$) are similar,[16] with the difference that only NCCS is bent.

Additional spectroscopic measurements of bent HC_4O and the three new chains reported here are needed to further clarify the structure of these radicals. Detection of $K_a=\pm 1$ transitions of HC_4O would provide information on its molecular geometry and planarity, and from the spin-rotation coupling constant ϵ_{aa}, the energy gap between the Renner-Teller pair can be estimated via the Curl relation.[20] For the linear chains, detection of transitions from the higher fine-structure level would enable the spin-orbit coupling constant to be determined indirectly by fitting a theoretical spectrum generated from an effective Hamiltonian[22–24] to the observed data. Most of these data can probably be best obtained at millimeter wavelengths using a long-path dc glow discharge source similar to the one used to detect HC_3O (Ref. 28) and other reactive molecules. This source is characterized by a high effective temperature ($T\sim 200-300$ K) in which high-lying rotational, vibrational, and fine-structure levels are thermally populated.

Isotopic measurements of the HC_nO radicals would provide definitive information on the molecular structure and the location of the unpaired electron along each chain and might help clarify the formation mechanism. For HC_4O, a determination of the bond angles in the heavy-atom backbone will allow one to determine whether this chain has an acetylene-type structure in which the CCO unit is bent or a cumulene-type structure in which the CCH unit is bent. The location of the unpaired electron in each radical can be derived from the analysis of carbon-13 hfs at each carbon atom along the chain. In the closely related C_nH chains, this structure shows that the unpaired electron is localized primarily at the terminal carbon atom and at alternating carbon atoms along the chain. Because the hydrogen coupling constants for HC_nO are quite similar to those of similarly sized C_nH radicals, one might expect that the unpaired electron is distributed along the chain in a similar way. Finally, comparing the line intensities of different carbon-13 isotopic species using isotopically enriched samples of ^{13}CO and other precursor gases might provide insight into the relative contributions of addition and other reactions to the overall HC_nO abundance.

Isotopic measurements can probably be undertaken with present instrumentation because the lines of several of the radicals are so intense in our spectrometer that the carbon-13 isotopic species can be observed in natural abundance; if not, detection of these species should be fairly routine using commercially available isotopically enriched samples. For the ^{18}O and deuterated species, strong lines can be readily produced using C ^{18}O and DCCD or DC_4D. Isotopic species of HC_4O and HC_5O are obvious candidates for detection, but those of HC_6O and HC_7O are probably also within reach.

Detection of still longer HC_nO radicals may be possible. Both HC_8O and HC_9O are good candidates because their line intensities, extrapolated from the shorter members of the sequence, are five times greater than our current detection

limit. Both chains are expected to possess linear heavy-atom backbones, $^2\Pi$ electronic ground states, and comparable dipole moments to those of the shorter chains. A large search in frequency is probably not required: rotational constants can probably be estimated to better than 1% by extrapolation (see Table I), on the assumption that the scaling factor (1.032) derived for the shorter chains is independent of chain length.

ACKNOWLEDGMENTS

We thank A. J. Apponi for assistance with some of the early experiments here, J. Dudek for the synthesis of precursor gases, and C. A. Gottlieb for several helpful discussions. The experimental work has been supported by the NASA Grant No. NAG5-9379, NSF Grants No. AST-9820722 and No. CHE-0353693, and the theoretical work by NSF Grant No. CHE-0216563.

[1] A. G. Gaydon, *The Spectroscopy of Flames* (Chapman and Hall, London, 1957).
[2] C. R. Lander, K. G. Unfried, G. P. Glass, and R. J. Curl, Jr., J. Chem. Phys. **94**, 7749 (1990).
[3] B.-M. Hass, T. K. Minton, P. Felder, and R. J. Curl, Jr., J. Chem. Phys. **95**, 5149 (1991).
[4] L. E. Snyder, M. S. Schenewerk, and J. M. Hollis, Astrophys. J. **298**, 360 (1985).
[5] N. G. Adams, D. Smith, K. Giles, and E. Herbst, Astron. Astrophys. **220**, 269 (1989).
[6] E. Hirota, *High-Resolution Spectroscopy of Transient Molecules* (Springer-Verlag, Berlin, 1985), pp. 47–61.
[7] I. C. Bowater, J. M. Brown, and A. Carrington, Proc. R. Soc. London, Ser. A **333**, 265 (1973).
[8] Y. Endo and E. Hirota, J. Chem. Phys. **86**, 4319 (1986).
[9] A. L. Cooksy, J. K. G. Watson, C. A. Gottlieb, and P. Thaddeus, J. Chem. Phys. **101**, 178 (1994).
[10] H. Kohguchi, Y. Ohshima, and Y. Endo, J. Chem. Phys. **101**, 6463 (1994).
[11] M. C. McCarthy, W. Chen, M. J. Travers, and P. Thaddeus, Astrophys. J., Suppl. Ser. **129**, 611 (2000).
[12] M. C. McCarthy and P. Thaddeus, Chem. Soc. Rev. **30**, 177 (2001).
[13] C. A. Gottlieb, A. J. Apponi, M. C. McCarthy, P. Thaddeus, and H. Linnartz, J. Chem. Phys. **113**, 1910 (2000).
[14] W. Chen, S. E. Novick, M. C. McCarthy, M. J. Travers, C. A. Gottlieb, A. L. Cooksy, and P. Thaddeus, Astrophys. J. **462**, 561 (1996).
[15] M. C. McCarthy and P. Thaddeus, J. Chem. Phys. **122**, 174308 (2005).
[16] M. W. Schmidt, K. K. Baldridge, J. J. Boatz, *et al.*, J. Comput. Chem. **14**, 1347 (1993).
[17] M. J. Frisch *et al.*, Gaussian 98, Revision A.6, Gaussian, Inc., Pittsburgh, PA, 1998.
[18] H. Wang and A. L. Cooksy, Chem. Phys. **213**, 139 (1996).
[19] M. C. McCarthy, A. L. Cooksy, S. Mohamed, V. D. Gordon, and P. Thaddeus, Astrophys. J., Suppl. Ser. **144**, 287 (2003).
[20] R. F. Curl, Jr., Mol. Phys. **9**, 585 (1965).
[21] See EPAPS Document No. E-JCPSA6-123-004543 for complete lists of experimental transition frequencies. This document can be reached via a direct link in the online article's HTML reference section or via the EPAPS homepage (http://www.aip.org/pubservs/epaps.html).
[22] J. M. Brown, M. Kaise, C. M. L. Kerr, and D. J. Milton, Mol. Phys. **36**, 553 (1978).
[23] J. M. Brown, E. A. Colbourn, J. K. G. Watson, and F. D. Wayne, J. Mol. Spectrosc. **74**, 294 (1979).
[24] C. Amiot, J.-P. Maillard, and J. Chauville, J. Mol. Spectrosc. **87**, 196 (1981).
[25] H. Lefebvre-Brion and R. W. Field, *Pertubations in the Spectra of Diatomic Molecules* (Academic, Boston, 1986), p. 214.
[26] M. C. McCarthy, W. Chen, A. J. Apponi, C. A. Gottlieb, and P. Thaddeus, Astrophys. J. **520**, 158 (1999).
[27] C. A. Gottlieb, M. C. McCarthy, M. J. Travers, J.-U. Grabow, and P. Thaddeus, J. Chem. Phys. **109**, 5433 (1998).
[28] M. C. McCarthy, C. A. Gottlieb, A. L. Cooksy, and P. Thaddeus, J. Chem. Phys. **103**, 7779 (1995).